

Synthesis, thermal and spectral studies of first-row transition metal complexes with Girard-T reagent-based ligand

Usama El-Ayaan ^{*}, I.M. Kenawy, Y.G. Abu El-Reash

Department of Chemistry, Faculty of Science, Mansoura University, Mansoura 35516, Egypt

Received 24 November 2006; received in revised form 22 January 2007; accepted 24 January 2007

Available online 1 February 2007

Abstract

The complexing behaviour of 1-acetyltrimethyl ammonium chloride-4-benzoyl thiosemicarbazide (H₂GTBzIT) towards the following first-row transition metal ions namely, Cr(III), Mn(II), Co(II), Ni(II), Cu(II) and Zn(II) have been examined by elemental analysis, magnetic measurements, electronic, IR and ¹H NMR. The proton-ligand ionization constants were determined potentiometrically using Irving–Rossotti technique. The stability constants of complexes were also calculated and were found in agreement with the sequence of stability constants of Irving and Williams. Thermal properties and decomposition kinetics of all complexes are investigated. The interpretation, mathematical analysis and evaluation of kinetic parameters (*E*, *A*, ΔH , ΔS and ΔG) of all thermal decomposition stages have been evaluated using Coats–Redfern and Horowitz–Metzger equations.

© 2007 Elsevier B.V. All rights reserved.

Keywords: Synthesis; Spectroscopic; Thermal degradation kinetics; Girard-T derivative

1. Introduction

The water-soluble properties of Girard-T hydrazones make the reagent potentially effective for isolation of carbonyls from mixtures soluble in non-polar solvents [1]. In work on the chemistry of rancidity [2], Gaddis et al. have found the reagent useful in learning about the distribution of volatile and non-volatile carbonyls in rancid fat. This work indicated possible usefulness of the reagent for investigation of the complex carbonyl anatomy of autoxidized fats. Successful application depends on adaptation to quantitative isolation of very small amounts of carbonyls, and on devising means of controlling the reaction so as to isolate at will free carbonyl and bound or potential carbonyl [3]. Recently, Girard-T reagent was applied as a very simple and efficient classical method for the purification of 3-aminoestrone. By this rapid procedure the purity of crude 3-aminoestrone was increased from 67% to 96% [4].

Finally, in view of the fact that these reagents and their Schiff bases possess ligating atoms they have also been studied as ligands in coordination chemistry [5,6].

In this paper we report the syntheses, spectral and thermogravimetric studies of new series of transition metal complexes of 1-acetyltrimethyl ammonium chloride-4-benzoyl thiosemicarbazide (H₂GTBzIT). The decomposition kinetics has been studied by employing the two methods viz. Coats–Redfern and Horowitz–Metzger. Thermodynamic parameters (ΔS , ΔH and ΔG), for each step of degradation have been calculated using the standard equations. In solution, ligand formation constants and stability constants of all studied complexes were determined potentiometrically using Irving–Rossotti technique.

2. Theoretical

2.1. Thermal degradation kinetics

Non-isothermal methods have been extensively used for the evaluation of kinetic parameters of decomposition

^{*} Corresponding author.

E-mail address: usama@mans.edu.eg (U. El-Ayaan).

reactions. The rate of decomposition process can be described as the product of two separate functions of temperature and conversion.

$$\frac{d\alpha}{dt} = k(T)f(\alpha) \quad (1)$$

where α is the fraction decomposed at time t , $k(T)$ is the temperature dependent function and $f(\alpha)$ is the conversion function dependent on the mechanism of decomposition. It has been established that the temperature dependent function $k(T)$ is of the Arrhenius type and can be considered as the rate constant k :

$$k = Ae^{-E/RT} \quad (2)$$

where R is the gas constant in ($\text{J mol}^{-1} \text{K}^{-1}$). Substituting Eq. (2) into Eq. (1), we get

$$d\alpha/dt = (A/\varphi e^{-E/RT})f(\alpha) \quad (3)$$

where φ is the linear heating rate dT/dt . On integration and approximation, this equation can be obtained in the following form:

$$\ln g(\alpha) = -E/RT + \ln(AR/\varphi E) \quad (4)$$

where $g(\alpha)$ is a function of α dependent on the mechanism of the reaction. The integral on the right hand side is known as temperature integral and has no closed form solution. Several techniques have been used for the evaluation of temperature integral. Most commonly used methods for this purpose are the differential method of Freeman–Carroll [7], integral method of Coats–Redfern [8], the approximation method of Horowitz–Metzger [9].

In the present investigation, kinetic parameters have been evaluated using the following two methods and results obtained are compared with one another.

2.1.1. Coats–Redfern equation

The Coats–Redfern equation, which is a typical integral method, can be represented as

$$\int_0^\infty d\alpha(1-\alpha)^n = (A/\varphi) \int_{T_1}^{T_2} e^{-E/RT} dt \quad (5)$$

For convenience of integration the lower term T_1 is usually taken as zero. This equation on integration gives,

$$\ln[-\ln(1-\alpha)/T^2] = -E/RT + \ln[AR/\varphi E] \quad (6)$$

A plot of left-hand side (LHS) against $1/T$ was drawn. E was calculated from the slope and A from the intercept value. The entropy of activation ΔS was calculated by using the equation:

$$\Delta S = R[\ln(Ah/kT_s)] \quad (7)$$

where k is the Boltzmann's constant and h is the Planck's constant and T_s is the DTG peak temperature [10].

The other kinetic parameters, ΔH and ΔG were computed using the relationships; $\Delta H = E - RT$ and $\Delta G = \Delta H - T\Delta S$.

2.1.2. Horowitz–Metzger equation

The Horowitz–Metzger equation is an illustrative of the approximation methods. These authors derived the relation:

$$\log\left\{[1 - (1-\alpha)^{1-n}]/(1-n)\right\} = E\theta/2.303RT_s^2 \text{ for } n \neq 1 \quad (8)$$

When $n = 1$, the LHS of Eq. (8) would be $\log[-\log(1-\alpha)]$. For first-order kinetics process the Horowitz–Metzger equation maybe written in the form:

$$\log[\log(w_x/w_y)] = E\theta/2.303RT_s^2 - \log 2.303 \quad (9)$$

where $\theta = T - T_s$, $w_y = w_x - w$, w_x is the mass loss at the completion of the reaction, and w is the mass loss up time t . The plot of $\log[\log(w_x/w_y)]$ versus θ was drawn and found to be linear from the slope of which E was calculated.

Other kinetic parameters ΔH , ΔS and ΔG were calculated as stated earlier in Section 2.1.1.

2.2. Molecular modeling

An attempt to gain a better insight on the molecular structure of ligand and its complexes, geometry optimization and conformational analysis has been performed by the use of MM+ [11] forcefield as implemented in hyperchem 5.1 [12].

3. Experimental

3.1. Instrumentation and materials

All starting materials were purchased from Fluka, Riedel and Merk and used as received. Elemental analyses (C, H, N) were performed on a Perkin-Elmer 2400 Series II Analyzer. Electronic spectra were recorded on a UV-UNICAM 2001 spectrophotometer using 10 mm pass length quartz cells at room temperature. Magnetic susceptibility was measured with a Sherwood Scientific magnetic susceptibility balance at 297 K. Infrared spectra were recorded on a Perkin-Elmer FT-IR Spectrometer 2000 as KBr pellets and as Nujol mulls in the 4000–370 cm^{-1} spectral range. ^1H NMR measurements at room temperature were obtained on a Jeol JNM LA 300 WB spectrometer at 400 MHz, using a 5 mm probe head in CDCl_3 . Chemical shifts are given in ppm relative to internal TMS (tetramethylsilane). Thermogravimetric (TG) and differential (DTG) thermogravimetric analysis were performed on a DTG-50 Shimadzu instrument at heating rate of 15 $^\circ\text{C}/\text{min}$.

3.2. Synthesis of 1-acetyl trimethylammonium chloride-4-benzoyl thiosemicarbazide

Preparation of 1-acetyl trimethylammonium chloride-4-benzoyl thiosemicarbazide (H_2GTBzIT) was carried out by refluxing (5.0 g, 30 mmol) of Girard-T with (4 ml, 30 mol) of benzoyl isothiocyanate in 20 ml absolute ethanol over a water bath for 4 h. The reaction mixture was left to cool till

white crystals were separated out. These were filtered off, recrystallized from ethanol and finally dried in vacuum desiccators over anhydrous calcium chloride; m.p. 192.3.

Yield: 8.0 g (80.6 %) of (H₂GTBzIT). Found: C, 46.90; H, 5.65; N, 15.95; S, 9.59. Calcd. for C₁₃H₁₉ClN₄O₂S (330.83): C, 47.2; H, 5.79; N, 16.94; S, 9.69%.

3.3. Synthesis of metal complexes

All complexes were prepared by refluxing H₂GTBzIT (0.33 g, 1.0 mmol) and the hydrated metal salts (1.0 mmol), e.g. chloride and acetate, in 30 ml ethanol for 2–3 h. The resulting solid complexes were filtered while hot, washed with ethanol followed by diethyl ether and dried in vacuo over CaCl₂.

4. Results and discussion

The analytical and physical data of (H₂GTBzIT) ligand and its complexes are listed in Table 1.

4.1. IR and NMR spectra of H₂GTBzIT ligand and its complexes

The principle IR bands of H₂GTBzIT and its metal complexes are listed in Table 2.

IR spectra (KBr) of H₂GTBzIT, show a three bands at 3151, 3099 and 3061 cm⁻¹ assigned to νNH(2), νNH(4) and νNH(1) modes, respectively. The two strong bands at 1689 and 1671 cm⁻¹ are attributed to ν(CO) groups of the hydrazide(h) and benzoyl(b) moieties, respectively. Also, two bands at 706 and 1221 cm⁻¹ are assigned to ν(CS) and a combination of (νCS + νCN) [13,14], respectively. The medium intensity band at 926 cm⁻¹ is attributed to the ν(N–N) vibration [15]. The sharp band at 3416 cm⁻¹ assigned to ν(OH) indicates the presence of H₂GTBzIT in the keto–enol form through CO group of benzoyl moiety (Fig. 1). This band is absent in the spectrum of (carboxymethyl) trimethyl ammonium chloride hydrazide (GT).

The NMR spectrum of H₂GTBzIT in DMSO-*d*₆, shows three signals at δ = 8.053, 8.025 and 8.023 ppm relative to TMS which disappear upon adding D₂O and can be assigned to NH(2), NH(4), NH(1) protons, respectively. The multiple at (7.90–7.49 ppm) is assigned to phenyl ring protons. The signal of CH₂ protons appears shifted to down field (5.05 ppm) because the presence of the quaternary nitrogen (N⁺) which act as a strong electron withdrawing group.

The IR spectrum of the [Cd(H₂GTBzIT)Cl₂·(H₂O)]·2H₂O complex shows that the ligand behaves as a neutral tridentate *via* the carbonyl oxygen (CO) of both hydrazide and benzoyl moieties in the keto form and the nitrogen of the NH group (Fig. 2). The mode of complexation is suggested by the shift of both ν(CO) and ν(NH) vibrations to higher wavenumber. Also, the ν(CS) shifted to higher wavenumber indicating that (CS) is out of coordination. The NMR spectrum of this complex shows a sig-

nal in the down-field region at δ = 11.7 ppm assigned to the coordinated (NH) proton and the signals of the other (NH) protons shifted to the higher field region 7.9–7.6 ppm may be due to break down of the hydrogen bond.

In the [Mn(H₂GTBzIT)₂Cl₂] complex, the ligand behaves as a neutral bidentate in both keto and enol form. In the keto form, H₂GTBzIT coordinate *via* CS in the thione form and CO of benzoyl moiety but in the enol form coordinate *via* the CS in the thione form and the nitrogen of NH(1) group (Fig. 3). This mode of coordination is supported by the following observations: the shift of both ν(CO) benzoyl and ν(CS) to lower wave number, ν(CO) of hydrazide moiety and ν(OH) of the enolized benzoyl moiety remains unchanged with simultaneous appearance of new bands at 1643 and 1110 cm⁻¹ assignable to ν(C=N) and ν(C–O), respectively.

In the [Cr(HGTBzIT)Cl₂(H₂O)]·2H₂O complex, H₂GTBzIT behaves as a mononegative tridentate coordinating through the CO of hydrazide moiety in the keto form, the nitrogen of the NH group and the enolic oxygen of the benzoyl moiety with the displacement of a hydrogen atom from the latter group as in (Fig. 4). This behavior is revealed by the disappearance of ν(CO) benzoyl moiety, νNH(4) and the great change in both the intensity and the position of ν(CO) of the hydrazide moiety with appearance of new bands assignable to ν(C–O) and ν(C=N).

H₂GTBzIT behaves as a binategative tridentate in the [Ni(GTBzIT)(H₂O)₃]·2H₂O and [Co₂(HGTBzIT)Cl₂·(H₂O)₃]·H₂O through the enolic oxygen of both carbonyl groups with the displacement of hydrogen atoms and the nitrogen of NH group. This behavior is revealed by the disappearance of ν(CO) benzoyl, ν(CO) hydrazide, νNH(4) and νNH(1) with appearance of new bands assignable to ν(C–O), νC=N(4) and νC=N(1). After heating the Ni(II) complex in vacuum oven at 120 °C for 6 h, the mass loss is about 7.74% which suggests that a two water molecules are uncoordinated.

In the [M₃(HGTBzIT)(GTBzIT)Cl₃(H₂O)₃] complexes where M = Cu(II) or Zn(II), ligand behaves as a mononegative and binategative tridentate. In the binategative, the ligand coordinates *via* the enolized oxygen of both CO with displacement of hydrogen atoms and NH group. The mononegative ligand coordinate *via* the enolized (CO) of hydrazide moiety with displacement of hydrogen atom, NH and the oxygen of CO of benzoyl in Zn(II) complex and the enolized oxygen of CO of benzoyl in Cu(II) complex without displacement of hydrogen atom.

4.2. Electronic spectra and magnetic moments of complexes

Electronic spectra were measured in 10⁻³ M dimethyl sulfoxide (DMSO) solution of all studied complexes. The band positions, magnetic moments and calculated ligand field parameters are given in Table 3.

The electronic spectrum of [Cr(HGTBzIT)Cl₂·(H₂O)]·2H₂O shows two strong absorption bands at 16,447 (ν₁) and 22,075 cm⁻¹ (ν₂). We could not observe

Table 1
Analytical and physical data of H₂GTBzIT ligand and its metal complexes

Compound	F.Wt	Color	Found (Calcd.) %						
			C	H	N	S	M	Cl	
H ₂ GTBzIT C ₁₃ H ₁₉ ClN ₄ O ₇ S	330.83	Green	46.90 (47.20)	5.65 (5.79)	15.95 (16.94)	9.59 (9.69)	–	–	
[Mn(H ₂ GTBzIT) ₂ Cl ₂] C ₂₆ H ₃₈ Cl ₄ MnN ₈ O ₁₄ S ₂	787.51	White	45.31 (39.66)	3.96 (4.86)	14.05 (14.23)	8.21 (8.14)	6.81 (6.98)	17.90 (18.00)	
[Cr(HGTBzIT)Cl ₃ (H ₂ O)] ₂ ·2H ₂ O C ₁₃ H ₂₄ Cl ₃ CrN ₄ O ₅ S	506.77	Green	30.1 (30.81)	4.47 (4.77)	11.20 (11.06)	6.63 (6.33)	9.94 (10.26)	20.35 (20.99)	
[Co ₂ (HGTBzIT)Cl ₂ (H ₂ O) ₃](H ₂ O) C ₁₃ H ₂₅ Cl ₃ Co ₂ N ₄ O ₆ S	589.65	Blue	26.30 (26.48)	4.12 (4.27)	9.03 (9.50)	5.63 (5.44)	20.12 (19.99)	18.23 (18.04)	
[Zn ₃ (HGTBzIT)(GTBzIT)Cl ₃ (H ₂ O) ₃] C ₂₆ H ₄₁ Cl ₃ N ₈ O ₇ S ₂ Zn ₃	1015.22	Gray	37.22 (37.02)	3.68 (3.73)	11.30 (11.51)	6.69 (6.54)	13.51 (13.43)	14.62 (14.57)	
[Ni(GTBzIT)(H ₂ O) ₃] ₂ ·2H ₂ O C ₁₃ H ₂₇ ClN ₄ NiO ₇ S	477.59	Pale-brown	32.2 (32.69)	5.61 (5.7)	11.32 (11.73)	6.64 (6.71)	12.80 (12.29)	7.13 (7.42)	
[Cu ₃ (HGTBzIT)(GTBzIT)Cl ₃ (H ₂ O) ₃] C ₂₆ H ₄₁ Cl ₃ Cu ₃ N ₈ O ₇ S ₂	1009.69	Deep-green	31.12 (30.93)	4.03 (4.09)	9.98 (11.1)	6.05 (6.35)	19.12 (18.88)	18.01 (17.56)	
[Cd(H ₂ GTBzIT)(H ₂ O) ₂] ₂ ·2H ₂ O C ₁₃ H ₂₅ Cl ₃ CdN ₄ O ₅ S	568.20	White	27.8 (27.48)	4.41 (4.43)	8.96 (9.86)	5.32 (5.64)	19.54 (19.78)	18.32 (18.72)	

the expected ν_3 band on our instrument which might be hidden below ν_2 . The three spin-allowed transitions for chromium(III) in an octahedral field are as follows: ${}^4A_{2g}(F) \rightarrow {}^4T_{2g}(F)$ (ν_1), ${}^4A_{2g}(F) \rightarrow {}^4T_{1g}(F)$ (ν_2) and ${}^4A_{2g}(F) \rightarrow {}^4T_{1g}(P)$ (ν_3). The ν_1 transition is a direct measurement of the ligand field parameter 10 Dq. From ν_1 and ν_2 , the value of B and β can be calculated. In addition, the μ_{eff} -value can be taken as additional evidence for the octahedral geometry [16].

The electronic spectrum of the [Mn(H₂GTBzIT)₂Cl₂] complex shows a strong band at 24,134 cm⁻¹ which is assigned to the ${}^6A_{1g} \rightarrow {}^4T_{2g}(D)$ transition. The other characteristic bands for d–d transitions are difficult to recognize in this complex and thus the ligand field parameters could not be calculated.

The nickel complex namely, [Ni(GTBzIT)(H₂O)₃].2H₂O shows spectral bands in the 14,577–17,391 and 26,246 cm⁻¹ regions, assignable to the ${}^3A_{2g} \rightarrow {}^3T_{1g}(F)$ (ν_2) and ${}^3A_{2g} \rightarrow {}^4T_{1g}(P)$ (ν_3) transitions, respectively indicating octahedral geometry.

The electronic spectrum of the blue complex, [Co₂(HGTBzIT)Cl₂(H₂O)₃].H₂O exhibits an intense band at 14,663 cm⁻¹ assignable to the ${}^4A_2(F) \rightarrow {}^4T_1(P)$ transition and a shoulder at 16,260 cm⁻¹ due to spin coupling, indicating tetrahedral geometry for this complex. The blue color as well as the magnetic moment of 3.77 B.M. are a further indication for the tetrahedral geometry [17].

The lowering in μ_{eff} (1.46 B.M.) of the trinuclear copper complex, [Cu₃(H GTBzIT)(GTBzIT)Cl₃(H₂O)₃] may be attributed to the covalent nature of the copper–sulphur bond. The electronic spectra show bands at 12,658, 20,000, 25,974 and 27,777 cm⁻¹ regions. These band positions are in agreement with those generally observed for square-planar copper(II) complexes [18,19].

4.3. Potentiometric studies

4.3.1. Determination of the proton-ligand ionization constants

The ionization constants of 1-acetyltrimethyl ammonium chloride-4-benzoyl thiosemicarbazide (H₂GTBzIT) was determined potentiometrically using Irving-Rossotti technique [20] at different temperatures (295, 308 and 318 K) and at constant ionic strength of 0.08 M KCl. At constant temperature of 295 K, the effect of different ionic strength on the proton-ligand ionization constant was studied using five different KCl concentrations. The ligand was titrated against carbonate-free sodium hydroxide (0.0105 M) solution.

The average number of protons associated with the ligand \bar{n}_A was calculated at different pH-values using Irving–Rossotti equation [20].

$$\bar{n}_A = Y - \frac{VN}{(V_0 - V)T_L}$$

Where Y is the ionizable protons in the ligand, V is the volume of the alkali at desired pH. V_0 is the initial volume of

Table 2
Infrared data (cm^{-1}) of H_2GTBzIT ligand and its metal complexes

Compound	IR (cm^{-1})						
	$\nu(\text{CO})_h$	$\nu(\text{CO})_b$	νCS	$\nu(\text{OH})$	$\nu(\text{N-N})$	$\nu(\text{C-O})$	$\nu(\text{C=N})$
H_2GPBzIT	1689	1671	706	3416	926	1080 sh	1640 sh
$[\text{Mn}(\text{H}_2\text{GTBzIT})_2\text{Cl}_2]$	1691	1665	703	3416	923	1100	1643
$[\text{Cr}(\text{HGTBzIT})\text{Cl}_2(\text{H}_2\text{O})]_2\text{H}_2\text{O}$	1670	–	714	–	971	1115	1621
$[\text{Co}_2(\text{HGTBzIT})\text{Cl}_2(\text{H}_2\text{O})_3]\text{H}_2\text{O}$	–	–	711	–	945	1105	1638
$[\text{Zn}_3(\text{HGTBzIT})(\text{GTBzIT})\text{Cl}_3(\text{H}_2\text{O})_3]$	–	1655 sh	712	–	924	1115	1601
$[\text{Ni}(\text{GTBzIT})(\text{H}_2\text{O})_3]_2\text{H}_2\text{O}$	–	–	713	–	934	1110	1645
$[\text{Ni}(\text{GTBzIT})(\text{H}_2\text{O})_3]_2\text{H}_2\text{O}$	–	–	713	–	934	1105	1636
$[\text{Cu}_3(\text{HGTBzIT})(\text{GTBzIT})\text{Cl}_3(\text{H}_2\text{O})_3]$	–	–	710	3331	937	1120	1605
$[\text{Cu}_3(\text{HGTBzIT})(\text{GTBzIT})\text{Cl}_3(\text{H}_2\text{O})_3]$	–	–	710	3331	937	1110	1626
$[\text{Cd}(\text{H}_2\text{GTBzIT})\text{Cl}_2(\text{H}_2\text{O})]_2\text{H}_2\text{O}$	1711	1676	711	–	921	1120	1601
$[\text{Cd}(\text{H}_2\text{GTBzIT})\text{Cl}_2(\text{H}_2\text{O})]_2\text{H}_2\text{O}$	1711	1676	711	–	921	–	–

b, benzoyl moiety.
h, hydrozide moiety.
sh, shoulder.

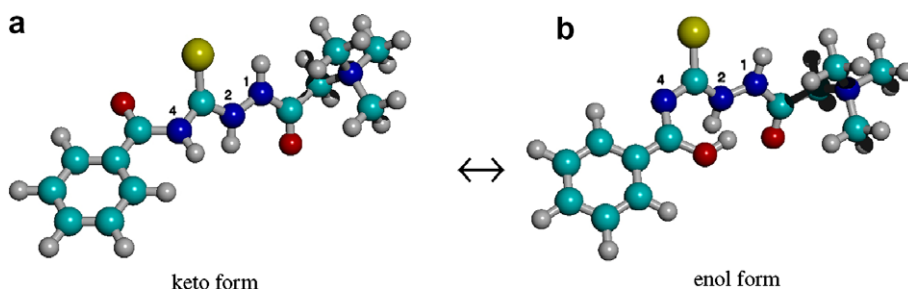


Fig. 1. Structure of the ligand (H_2GTBzIT).

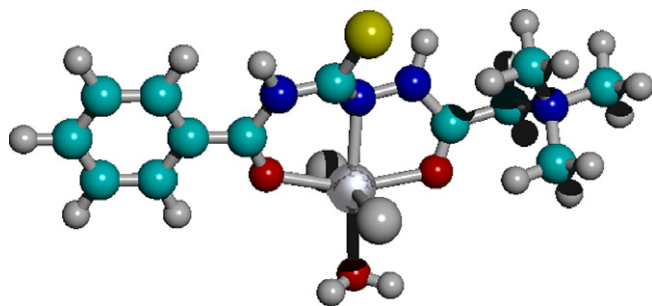


Fig. 2. Structure of $[\text{Cd}(\text{H}_2\text{GTBzIT})\text{Cl}_2(\text{H}_2\text{O})]_2\text{H}_2\text{O}$.

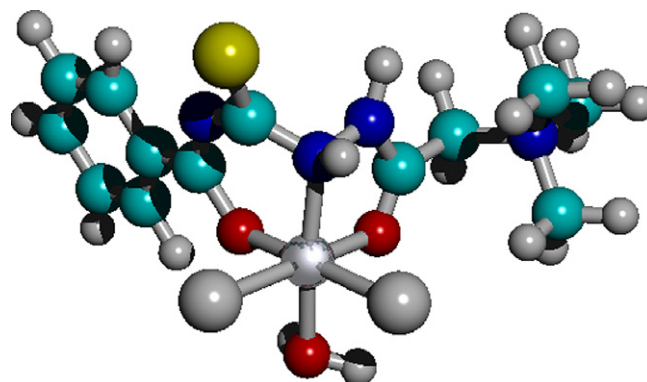


Fig. 4. Structure of $[\text{Cr}(\text{HGTBzIT})\text{Cl}_2(\text{H}_2\text{O})]_2\text{H}_2\text{O}$.

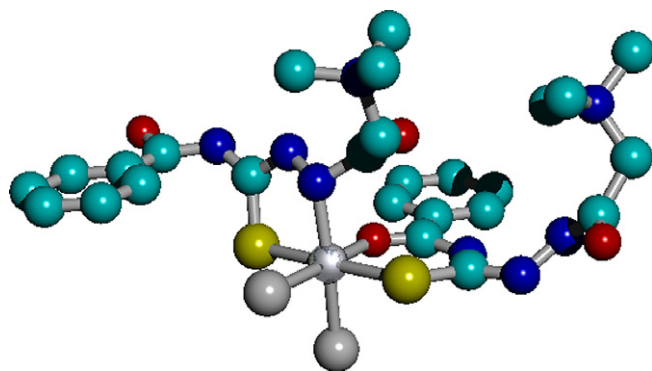


Fig. 3. Structure of $[\text{Mn}(\text{H}_2\text{GTBzIT})_2\text{Cl}_2]$.

the titrated mixtures (25 ml in this study), T_L is the initial ligand concentration, and N is the concentration of the alkali.

The proton-ligand formation curves are obtained by plotting \bar{n}_A versus pH. Same study was applied for other two temperatures namely, 308 and 318 K.

From these curves, the maximum \bar{n}_A value was found to be ~ 1 indicating the presence of one dissociable amide proton in the ligand.

The proton-ligand stability constant ($\text{p}K_a$) of H_2GTBzIT was determined by interpolation at half- \bar{n}_A val-

Table 3
Magnetic Moment, Electronic bands and ligand field parameters of the complexes derived from H₂GTBzIT

Compound ^a	Band position (cm ⁻¹)	Dq	B	β	μ _{eff} (B.M.)
[Cr(HGTBzIT)Cl ₂ (H ₂ O)]·2H ₂ O	16,447, 22,075, 25,641, 27,933	1644	539.1	0.59	3.89
[Mn(H ₂ GTBzIT) ₂ Cl ₂]	24,134, 25,413	–	–	–	7.30
[Ni(GTBzIT)(H ₂ O) ₃]·2H ₂ O	14,577, 17,391, 19,342, 26,246	759.4	1021	0.98	3.40
[Co ₂ (HGTBzIT)Cl ₂ (H ₂ O) ₃]·H ₂ O	14,663, 16,260, 19,120	–	–	–	3.77
[Cu ₃ (HGTBzIT)(GTBzIT)Cl ₃ (H ₂ O) ₃]	12,658, 20,000, 25,974, 27,777	–	–	–	1.46

^a Electronic spectra were measured in 10⁻³ M dimethyl sulphoxide (DMSO) solution of all studied complexes.

ues, i.e. at $\bar{n}_A = 0.5$ from the \bar{n}_A -pH curves. These values are confirmed by the method of least square by plotting $\log(\bar{n}_A/1 - \bar{n}_A)$ versus pH as shown in (Fig. 5).

The thermodynamic properties of solutions are not only useful for estimating the feasibility of reaction in solution, but they also offer one of the better methods for investigating the theoretical aspects of solution [21].

The standard free energy (ΔG°) associated with the acid dissociation can be calculated from the equilibrium constants of the reaction, as follow:

$$\Delta G^\circ = -2.303 RT \text{p}k_a$$

While the standard enthalpy change (ΔH°) of dissociation can be estimated from the use of Van't Hoff equation:

$$\frac{d \ln K}{dT} = \frac{\Delta H^\circ}{RT^2}$$

By plotting $\text{p}k_a$ versus $1/T$, from the slope the enthalpy change (ΔH°) for the dissociation of the ligand can be calculated.

Also, the standard entropy change (ΔS°) of dissociation can be calculated using the following well known equation:

$$\Delta G^\circ = \Delta H^\circ - T\Delta S^\circ$$

The stoichiometric thermodynamic functions are summarized in Table 4. From these data the following conclusions can be obtained:

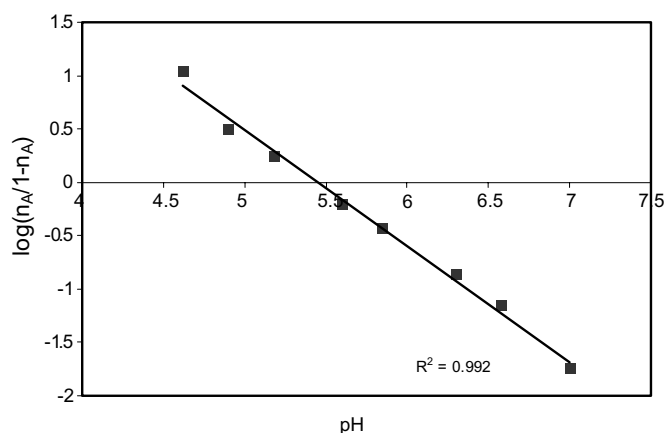


Fig. 5. Relation between $\log(\bar{n}_A/1 - \bar{n}_A)$ versus pH for proton-H₂GTBzIT, 0.20 M KCl and at 295 K.

Table 4
Thermodynamic parameters and association constant for H₂GTBzIT (0.08 M KCl) at different temperatures

Temperature (K)	p <i>k</i> _a	Δ <i>G</i> [°] (kJ mol ⁻¹)	-TΔ <i>S</i> [°] (kJ mol ⁻¹)	Δ <i>H</i> [°] (kJ mol ⁻¹)
295	5.30	29.94	14.73	15.21
308	5.05	29.78	14.57	
318	4.85	29.53	14.32	

- $\text{p}k_a$ values decrease with increasing temperature, i.e. the acidity of the ligand increases with increasing temperature Table 4.
- The positive values of ΔH indicate that the dissociation processes are endothermic in nature and enhance with the rise of temperature.
- The negative values of ΔS are owing to the increasing of the order as a result of solvation process, which can be explained as the sum of the bound solvent molecules with the dissociated ligand being more than the solvent molecules originally accompanying the un-dissociated form.
- ΔG values for the dissociation constants are positive, i.e. the dissociation processes are non-spontaneous.
- The correlations of $\text{p}k_a$ values versus $1/T$ are linear in all cases, suggesting that ΔC_p values for the dissociation processes are zero over the studied temperature range (295–318 K).

We also studied the effect of differing the ionic strength on the proton-ligand stability constant and the result indicate that the values of $\text{p}k_a$ of the ligand decrease as the ionic strength increases due to inert salt effect (Table 5).

4.3.2. Determination of stability constants of H₂GTBzIT complexes

First-row transition metal complexes with H₂GTBzIT ligand have been studied potentiometrically. These include, Cu(II), Co(II), Ni(II), Zn(II), Fe(III) in addition to Cd(II). The titrations were performed at different ionic strength

Table 5
The association constants of H₂GTBzIT

Method	<i>p</i> <i>k</i> _a (M)				
	0.04	0.08	0.12	0.16	0.20
Mid-point (half-method)	5.0	5.2	5.4	5.4	5.4
Least square method	5.05	5.3	5.4	5.4	5.4

values ranging from (0.04–0.20 M KCl) and at temperature of 295 K.

An inspection of the titration curves for H₂GTBzIT reveals that the metal-ligand titration curves are below and well separated from the ligand titration curves. This indicates that the complexation processes were occurred with liberation of hydrogen ions.

The stability constant are evaluated from the formation curves drawn between n and pL , where n is the average number of ligand attached per metal ion and pL is the free ligand exponent, n values can be calculated from the following equation:

$$\bar{n} = \frac{T_L - [L]}{T_M}$$

where T_L and T_M are the initial concentrations of the ligands and the metal, respectively, and $[L]$ is the ligand concentration at equilibrium. Therefore, the difference between T_L and $[L]$ is the concentration of the bound ligand to the metal ion. The above equation can rewrite as follow:

$$n = \frac{(V_2 - V_1)N^o}{(V_0 + V_1)n_A T_M}$$

where V_2 is the volume of alkali required to reach the desired pH in the mixture of complex solution, T_M is the initial metal ion concentration.

The pL value can be calculated by the following equation:

$$pL = \frac{\sum_{j=0}^{j=j} \beta_j H^j}{T_L - \bar{n}} * \frac{(V_2 + V_0)}{V_0}$$

and for monobasic acid the following simplified form of equation can successfully apply [22],

$$pL = pk_a - pH - \log\{[HA]_{\text{init}} - [OH^-]\}$$

The stoichiometric stability constants are evaluated using the half-method in which the following equation was applied:

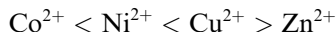
$$\log K = \log(1/[L])_{n=0.5}$$

(The pK values are evaluated at $n = 0.5$)

The experimental stability constant values (Table 6) for complexation of the investigated ligands were found follows the order:

Table 6
The stability constants of metal ions–H₂GTBzIT complexes at different ionic strength of KCl and at 295 K

Complex	pK (M)				
	0.04	0.08	0.12	0.16	0.20
Cu(II)–H ₂ GTBzIT	4.84	4.98	4.70	4.70	4.70
Co(II)–H ₂ GTBzIT	3.6	–	3.58	3.30	3.30
Ni(II)–H ₂ GTBzIT	4.14	4.42	4.00	4.00	4.00
Cd(II)–H ₂ GTBzIT	4.14	4.42	4.00	4.00	4.00
Zn(II)–H ₂ GTBzIT	2.90	2.40	2.32	2.30	2.30
Fe(III)–H ₂ GTBzIT	4.98	4.98	4.98	4.98	4.84



In agreement with the will known sequence of stability constants of Irving and Williams [23], clearly this order reflects the changes in heats of complexation along the series and it arises from the influence of the polarization ability of the metal ions, as measured by the ratio of charge to ionic radius.

Moreover, Irving and Williams series is a consequence of crystal-field stabilization energy which varies in the order of $\text{Co}^{2+} < \text{Ni}^{2+} < \text{Cu}^{2+} > \text{Zn}^{2+}$, i.e. the splitting caused by the ligand in the energy level of the d-electrons diminishes the total energy of the system, thus causes in stabilization.

Also the results show that the trivalent metal ions are more stable than that of divalent ones, as a result of increasing the oxidation state.

4.4. Thermal analysis

In studying the decomposition kinetics, many methods mentioned in literature were used [24–27]. In each case the least square plots were drawn. The first few points that did not fall on the straight line were discarded. These types of deviations were reported by several researches [28]. This is explained as due to the failure by obeying as first order kinetics always by the solids in their decomposition in the early stages. The TG/DTG curves (Fig. 6) of cadmium complex, $[\text{Cd}(\text{H}_2\text{GTBzIT})\text{Cl}_2(\text{H}_2\text{O})] \cdot 2\text{H}_2\text{O}$ are presented as a representative example.

The kinetic parameters evaluated by Coats–Redfern (CR) and Horowitz–Metzger (HM) methods are listed in Tables 7 and 8, respectively. In both methods, (CR and HM) the left hand side of equations 6 and 9 are plotted against $1000/T$ and θ , respectively (Fig. 7). From the results obtained, the following remarks can be pointed out: (i) The energy of activation (E) values increases on going from one decomposition stage to another for a given complex, indi-

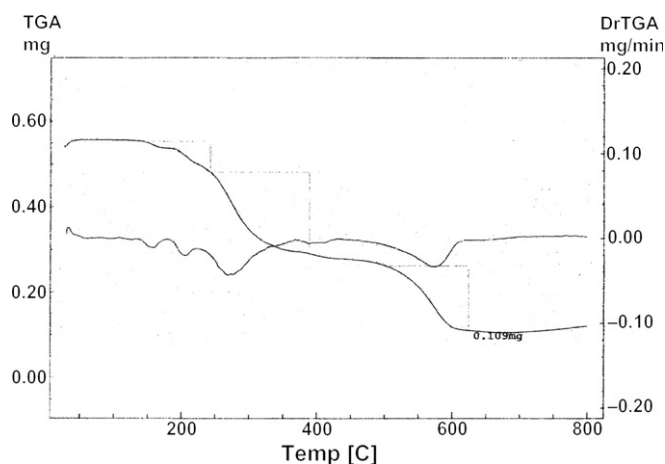


Fig. 6. TG and DTG of $[\text{Cd}(\text{H}_2\text{GTBzIT})\text{Cl}_2(\text{H}_2\text{O})] \cdot 2\text{H}_2\text{O}$.

Table 7
Kinetic parameters evaluated by Coats–Redfern equation

Compound	Stage	<i>T</i> (K)	<i>A</i> (S ⁻¹)	<i>E</i> (kJ mol ⁻¹)	ΔH (kJ mol ⁻¹)	ΔS (kJ mol ⁻¹ K ⁻¹)	ΔG (kJ mol ⁻¹)
[Cd(H ₂ GTBzIT)Cl ₂ (H ₂ O)]·2H ₂ O	1st	478	5.52 × 10 ⁵	72.8	68.8	-0.139	135
	2nd	555	11.9	37.4	32.8	-0.229	160
	3rd	837	1.66 × 10 ¹²	230.3	223.3	-0.020	240
[Co ₂ (HGTBzIT)Cl ₂ (H ₂ O) ₃]·H ₂ O	1st	614	33.6 × 10 ⁹	147.5	142.4	-0.049	173
	2nd	709	47.4 × 10 ⁷	159.8	153.9	-0.086	215
	3rd	878	22.2 × 10 ⁷	178.4	171.0	-0.094	254
[Cr(HGTBzIT)Cl ₂ (H ₂ O)]·2H ₂ O	1st	583	17.9 × 10 ⁴	83.9	86.1	-0.150	166
	2nd	658	21.1 × 10 ¹⁴	217.8	212.4	0.042	185
[Mn(H ₂ GTBzIT) ₂ Cl ₂]	1st	541	27.7 × 10 ²	59.9	55.4	-0.184	155
	2nd	659	82.1 × 10 ⁵	116.4	110.9	-0.119	189
	3rd	866	17.1 × 10 ⁴	127.8	120.6	-0.154	254
[Ni(GTBzIT)(H ₂ O) ₃]·2H ₂ O	1st	545	11.6 × 10 ⁷	106.4	101.9	-0.096	154
	2nd	655	85.0 × 10 ⁹	162.7	157.3	-0.042	185
	3rd	772	32.3 × 10 ¹⁰	202.0	196.0	-0.032	221
[Zn ₃ (HGTBzIT)(GTBzIT)Cl ₃ (H ₂ O) ₃]	1st	578	29.4 × 10 ⁵	95.8	91.0	-0.127	164
	2nd	733	6.66	50.0	43.9	-0.237	217
	3rd	921	32.3 × 10 ³	123.9	116.2	-0.168	271

Table 8
Kinetic parameters evaluated by Horowitz–Metzger equation

Compound	Stage	<i>T</i> (K)	<i>A</i> (S ⁻¹)	<i>E</i> (kJ mol ⁻¹)	ΔH (kJ mol ⁻¹)	ΔS (kJ mol ⁻¹ K ⁻¹)	ΔG (kJ mol ⁻¹)
[Cd(H ₂ GTBzIT)Cl ₂ (H ₂ O)]·2H ₂ O	1st	478	5.40 × 10 ⁵	87.3	83.4	-0.139	150
	2nd	555	12.2	34.8	30.1	-0.229	157
	3rd	837	1.71 × 10 ¹²	228.0	221.1	-0.019	237
[Co ₂ (HGTBzIT)Cl ₂ (H ₂ O) ₃]·H ₂ O	1st	614	34.0 × 10 ⁹	144.4	139.3	-0.049	173
	2nd	709	50.1 × 10 ⁷	137.6	131.7	-0.086	192
	3rd	878	19.2 × 10 ⁷	191.6	184.2	-0.095	268
[Cr(HGTBzIT)Cl ₂ (H ₂ O)]·2H ₂ O	1st	583	16.2 × 10 ⁴	91.0	79.0	-0.150	174
	2nd	658	22.3 × 10 ¹⁴	208.1	202.6	0.042	175
[Mn(H ₂ GTBzIT) ₂ Cl ₂]	1st	541	26.3 × 10 ²	72.8	68.3	-0.184	168
	2nd	659	80.4 × 10 ⁵	124.5	119.0	-0.119	197
	3rd	866	15.6 × 10 ⁴	143.4	136.1	-0.154	269
[Ni(GTBzIT)(H ₂ O) ₃]·2H ₂ O	1st	545	10.9 × 10 ⁷	113.7	109.2	-0.096	162
	2nd	655	84.8 × 10 ⁹	164.3	158.8	-0.042	186
	3rd	772	30.3 × 10 ¹⁰	228.2	221.8	-0.032	247
[Zn ₃ (HGTBzIT)(GTBzIT)Cl ₃ (H ₂ O) ₃]	1st	578	27.7 × 10 ⁵	108.5	103.7	-0.127	177
	2nd	733	6.33	51.4	45.3	-0.237	219
	3rd	921	35.0 × 10 ³	81.2	73.6	-0.167	228

cating that the rate of decomposition decreases in the same order. Generally stepwise stability constants decreases with an increase in the number of ligand attached to a metal ion. Conversely, during decomposition reaction the rate of removal of remaining ligands will be smaller after the expulsion of one or two ligands. (ii) The values of ΔG increases significantly for the subsequently decomposition stages due to increasing the values of (*T* ΔS) from one stage to another. This may be attributed to the structural rigidity of the remaining complex after the expulsion of one and more ligands, as compared with the precedent complex, which require more energy, *T* ΔS , for its rearrangement

before undergoing any compositional change. (iii) the negative ΔS values for the decomposition steps indicate that all studied complexes are more ordered in their activated states. (iv) the positive ΔH values mean that the decomposition processes are endothermic.

Conclusion

In solid state, the stability of complexes was examined and the kinetic parameters were evaluated using the Coats–Redfern method (a typical integral method) and the Horowitz–Metzger (an approximation method). The

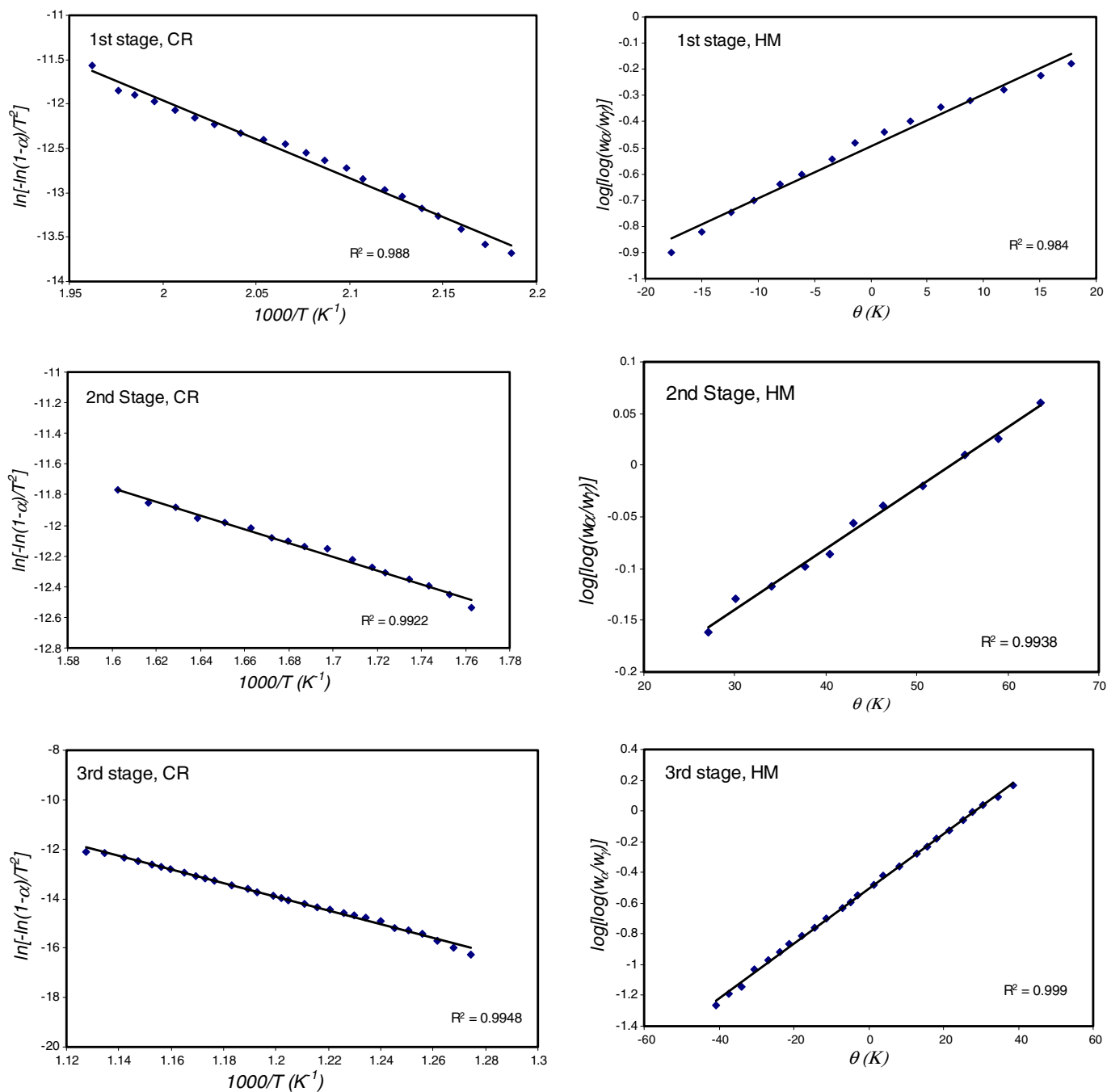


Fig. 7. Coats-Redfern (CR) and Horowitz-Metzger (HM) plots for $[\text{Cd}(\text{H}_2\text{GTBzIT})\text{Cl}_2(\text{H}_2\text{O})]\cdot 2\text{H}_2\text{O}$.

result shows that the kinetic parameters (E , ΔH , ΔS and ΔG) evaluated by both methods are in a very good agreement.

In solution, the stability constant of complexes was found follows the order: $\text{Co}^{2+} < \text{Ni}^{2+} < \text{Cu}^{2+} > \text{Zn}^{2+}$, in agreement with the will known sequence of stability constants of Irving and Williams.

References

- [1] A.M. Gaddis, R. Ellis, G.T. Currie, *Nature* 191 (1961) 1391.
- [2] A.M. Gaddis, R. Ellis, G.T. Currie *Food Res.* 25 (1960) 495.
- [3] A. Girard, G. Sandulesco, *Helv. Chim. Acta* 19 (1936) 1095.
- [4] I.-I. Radu, D. Poirier, L. Provencher, *Tetrahedron Lett.* 43 (2002) 7617.
- [5] X. Wang, X.M. Zhang, H.X. Liu, *Inorg. Chim. Acta* 223 (1994) 193.
- [6] X. Wang, X.M. Zhang, H.X. Liu, *J. Coord. Chem.* 33 (1994) 223.
- [7] E.S. Freeman, B. Carroll, *J. Phys. Chem.* 62 (1958) 394.
- [8] A.W. Coats, J.P. Redfern, *Nature* 201 (1964) 68.
- [9] H.H. Horowitz, G. Metzger, *Anal. Chem.* 35 (1963) 1464.
- [10] J.H.F. Flynn, L.A. Wall, *J. Res. Natl. Bur. Stand.* 70A (1996) 487.
- [11] N.L. Allinger, *J. Am. Chem. Soc.* 99 (1977) 8127.
- [12] HyperChem version 5.1 Hypercube, Inc.
- [13] C.N.R. Rao, R. Venkataraghavan, *Spectrochim. Acta* 18 (1962) 541.
- [14] Z. Li, Y. Zhang, Y. Wang, *Phosphorus, Sulfur Silicon Relat. Elem.* 178 (2003) 293.
- [15] D.N. Sathyanarayana, D. Nicholls, *Spectrochim. Acta Part A* 34 (1978) 263.

- [16] U. El-Ayaan, I.M. Kenawy, Y.G.A. El-Reash, *Spectrochim. Acta* (2006), doi:10.1016/2006.11.016.
- [17] L.H. Abdel-Rahman, *Transition Met. Chem.* 31 (2006) 943.
- [18] L. Sacconi, M. Ciampolini, *J. Chem. Soc.* (1964) 276.
- [19] U. El-Ayaan, G. Abu El-Reash, I.M. Kenawy, *Synth. React. Inorg. Met.-Org. Chem.* 33 (2003) 327.
- [20] H.M. Irving, H.S. Rossotti, *J. Chem. Soc.* (1954) 2904.
- [21] N.T. Abdel-Ghani, Y.M. Issa, M.A. Khaled, M.H. Kottany, *Thermochim. Acta* 125 (1988) 163.
- [22] A. Albert, E.P. Serjeant, *The Determination of Ionization Constants*, Chapman and Hall, London, 1971.
- [23] H.M. Irving, R.J.P. Williams, *J. Chem. Soc.* (1953) 3192.
- [24] T. Ozawa, *Bull. Chem. Soc. Jpn.* 38 (1965) 1881.
- [25] P. Kofstad, *Nature* 179 (1957) 1362.
- [26] H.H. Horowitz, G. Metzger, *Anal. Chem.* 35 (1963) 1464.
- [27] W.W. Wendlandt, *Thermal Methods of Analysis*, Wiley, New York, 1974.
- [28] V. Indira, G. Parameswaran, *J. Therm. Anal.* 29 (1984) 3.